

## Irradiation of Living Cells with Single Ions at the Ion Microprobe SNAKE

A. HAUPTNER<sup>a</sup>, T. CREMER<sup>b</sup>, M. DEUTSCH<sup>c</sup>, S. DIETZEL<sup>b</sup>,  
G.A. DREXLER<sup>c</sup>, C. GREUBEL<sup>a</sup>, V. HABLE<sup>d</sup>, R. KRÜCKEN<sup>a</sup>,  
R. LÖWE<sup>c</sup>, H. STRICKFADEN<sup>b</sup>, G. DOLLINGER<sup>d</sup> AND A.A. FRIEDL<sup>c</sup>

<sup>a</sup>Physik Department E12, Technische Universität, München, Germany

<sup>b</sup>Department Biologie II, Ludwig-Maximilians-Universität  
München, Germany

<sup>c</sup>Strahlenbiologisches Institut, Ludwig-Maximilians-Universität  
München, Germany

<sup>d</sup>Institut für Angewandte Physik und Messtechnik (LRT 2)  
Universität der Bundeswehr, München, Germany

The irradiation setup at the ion microprobe SNAKE is used to irradiate living cells with single energetic ions. The irradiation accuracy of  $0.55 \mu\text{m}$  and respectively  $0.40 \mu\text{m}$  allows to irradiate substructures of the cell nucleus. By the choice of ion atomic number and energy the irradiation can be performed with a damage density adjustable over more than three orders of magnitude. Immunofluorescence detection techniques show the distribution of proteins involved in the repair of DNA double-strand breaks. In one of the first experiments the kinetics of appearance of irradiation-induced foci in living HeLa cells was examined. In other experiments a new effect was detected which concerned the interaction between irradiation events performed at different time points within the same cell nucleus.

PACS numbers: 29.27.Eg, 61.80.Jh, 87.16.Sr, 87.50.Gi

### 1. Introduction

The ion microprobe SNAKE (superconducting nanoprobe for applied nuclear (**K**ern) physics experiments) enables to focus light and heavy ions delivered by the 14 MV Munich tandem accelerator. It is therefore a versatile instrument for the analysis and modification in material and biological sciences. One main application up to now is the three-dimensional hydrogen microscopy with sub-ppm detection limit [1]. Other current activities at the ion microprobe SNAKE concentrate on cell irradiation with single ions [2]. The relevant quantity for the damage

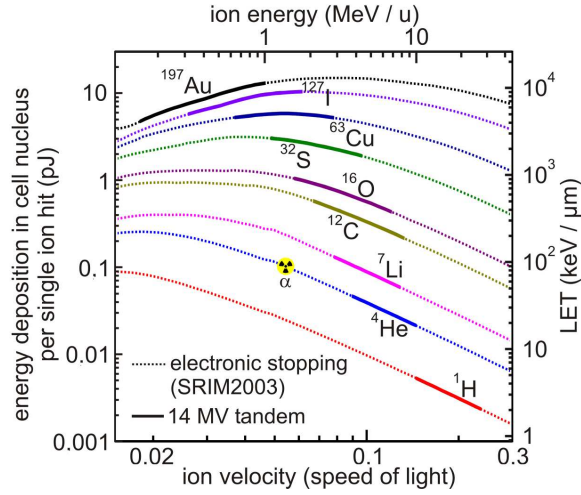


Fig. 1. Relationship between ion velocity and energy deposited in a cell nucleus per single ion hit. The continuous line sections mark the respective energy regions provided by the Munich 14 MV tandem accelerator.

induced in a living cell is the linear energy transfer (LET) value, which depends on atomic number and energy of the ion. Calculations of LET values were done using SRIM2003 software [3] assuming cell nuclei consisting of water. In Fig. 1 the corresponding relationship for a number of different ions is shown as well as the sections (= continuous line sections) supported by the 14 MV Munich tandem accelerator. It is evident that a variation of LET values over more than three orders of magnitude is possible, thus making cell irradiation experiments attractive.

## 2. Experimental technique

In order to focus the ion beam to a submicron beamspot, the ion microprobe SNAKE consists of a precision slit system and a superconducting magnetic lens

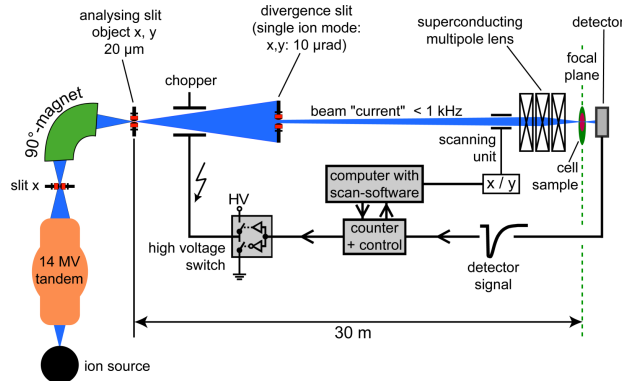


Fig. 2. Ion beam preparation and transport at the ion microprobe SNAKE.

(Fig. 2). The object micro-slits define the object for the ion-optical transformation and have an opening of  $20\ \mu\text{m}$  in  $x$ - and respectively  $10\ \mu\text{m}$  in  $y$ -direction. The divergence slits located at a distance of about  $5\ \text{m}$  determine the aperture of the ion beam and have an opening of typically  $60\ \mu\text{m}$  in both directions. The transmission through the whole micro-slit system amounts to less than  $10^{-8}$ , leading to a particle rate of a few hundreds per second. Due to the ion-optical geometry the superconducting lens provides a focussing action with demagnification factors of 88 in  $x$ - and 24 in  $y$ -direction. Thus a beam spot size well below  $0.5\ \mu\text{m}$  can be achieved. An electrostatic deflection system mounted in front of the magnetic lens allows to scan the ion beam at the focal plane without moving the target mechanically. In order to prepare single particles an electrostatic chopper system in front of the divergence slits acts as a fast beam shutter triggered by the hit signal from an ion detector at the target.

The cells to be irradiated are grown on a  $6\ \mu\text{m}$  thick mylar foil in a container made of stainless steel. Another  $6\ \mu\text{m}$  mylar foil acting as cover foil seals this cell chamber. During irradiation experiments the container is filled half with culture medium and put upright into the focal plane of the ion microprobe SNAKE. As can be seen in Fig. 3 the ion beam exits the vacuum of the beam transport system through a  $7.5\ \mu\text{m}$  thick Kapton foil which is in direct contact to the cell carrier foil from behind. Thus beam spot broadening by angular straggling effects can be minimized. The particle detector is mounted on the turret of an optical microscope situated behind the cell chamber. With the aid of this microscope the ion beam can be focussed during beam preparation and the cells can be observed before and after the irradiation procedure. To ensure proper operation of the irradiation setup and to obtain a measure for the irradiation resolution nuclear track detectors were irradiated using  $100\ \text{MeV O}$  ions. Figure 4 shows an irradiated matrix pattern with a pitch size of  $5\ \mu\text{m}$ . From the deviations between actual hit position and ideal hit position a resolution of  $0.55\ \mu\text{m}$  (FWHM) in  $x$ - and  $0.40\ \mu\text{m}$  (FWHM) in  $y$ -direction could be determined.

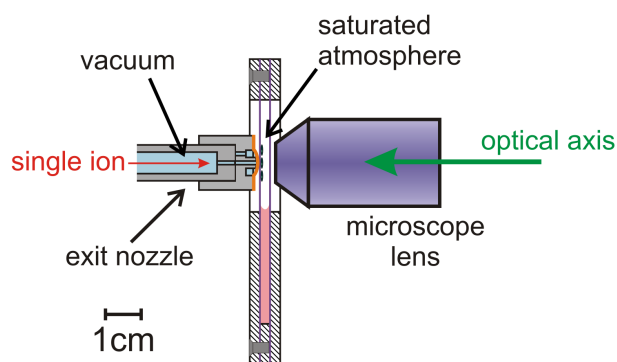


Fig. 3. Cell container in irradiation position. During irradiation the microscope objective is replaced by a particle detector.

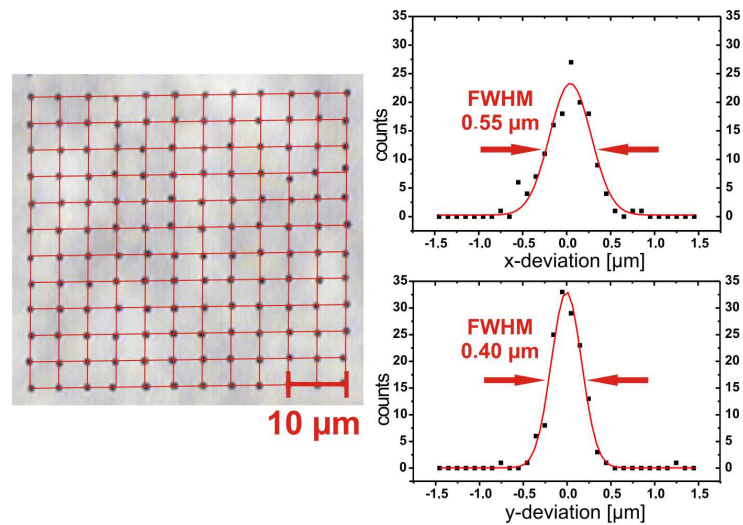


Fig. 4. Left side: irradiation test with single 100 MeV  $^{16}\text{O}$  ions using nuclear track detector foils. Right side: the irradiation resolution was determined to  $0.55\ \mu\text{m}$  (FWHM) in  $x$ - and respectively  $0.40\ \mu\text{m}$  (FWHM) in  $y$ -direction.

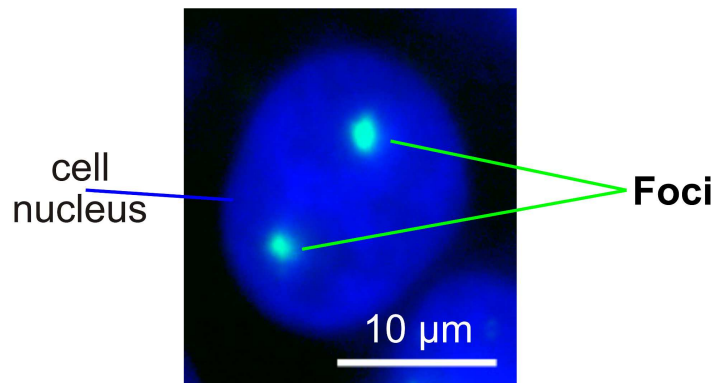


Fig. 5. Optical micrograph of a HeLa cell nucleus irradiated by two single 100 MeV  $^{16}\text{O}$  ions. The foci show the distribution of immunostained 53Bp1 protein.

The analysis of the irradiated cells is done by immunostaining techniques. For that purpose antibodies are allowed to enter the nuclei of the fixed cells. In a two step process, first primary antibodies bind specifically to selected proteins involved in the repair of DNA double-strand breaks (DSBs) before secondary antibodies labelled by a fluorescent dye bind to the first ones. In Fig. 5 an example of a cell nucleus irradiated by two single 100 MeV oxygen ions and prepared for 53Bp1 repair protein detection is shown. The corresponding foci clearly are visible. Nuclear DNA is counterstained with Dapi.

### 3. Results

In order to study the spatiotemporal dynamics of DNA DSB repair processes, living HeLa cells were irradiated using a line pattern consisting of single 100 MeV O ion hits separated by  $1\ \mu\text{m}$  in  $x$ - and  $6\ \mu\text{m}$  in  $y$ -direction. Several cell samples thus were irradiated and incubated afterwards for different time spans where repair could take place. Figure 6 shows two examples with incubation time of 0.5 hour and respectively 15 hours prepared for  $\gamma\text{H2AX}$  detection. By using “ROOT”-software package [4] the development of foci size and position in time was evaluated [5]. With increasing incubation time the foci positions showed an

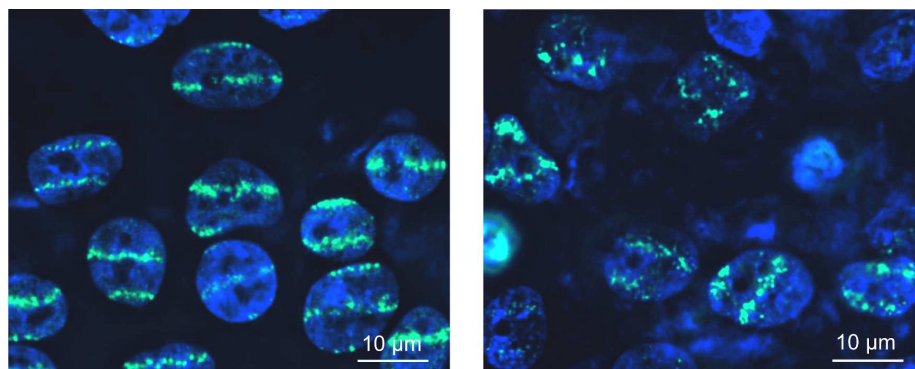


Fig. 6. HeLa cells irradiated by a line pattern consisting of single 100 MeV  $^{16}\text{O}$  ion hits. The time span between irradiation and observation was 0.5 hour (left side) and respectively 15 hours (right side). One can see an increased scatter of foci after the long time span.

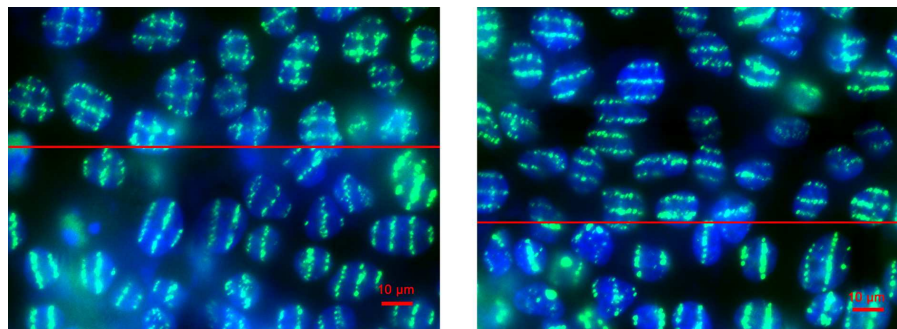


Fig. 7. Optical micrographs of irradiated HeLa cells showing “competition” effect in the distribution of 53Bp1 protein. Left side: cell nuclei with a time span of 15 min between first and second irradiation show 53Bp1 signal from all irradiation events. Right side: in cell nuclei with a time span of 45 min between the two irradiations the 53Bp1 signal is inhibited at the second irradiation due to the first irradiation (horizontal lines), while the cell nuclei only exposed to the second irradiation show clearly detectable 53Bp1 signal (vertical lines in the lower part of the image).

increasing scatter around the irradiated line compatible with a diffusion process. The foci size exhibited a more complex time behaviour, consisting of an initial increase and a following decrease after about 0.5 hour at the edge of the cell nucleus and respectively 2 hours at the centre of the cell nucleus. In another type of experiments a potential interaction between irradiation events separated in time within one cell nucleus was investigated. HeLa cells were irradiated twice with 100 MeV O ions forming defined irradiation patterns, so that foci formed after the first and after the second irradiation could be distinguished. We observed an inhibition of 53Bp1 protein accumulation after the second irradiation event in cells which were pre-irradiated about 45 min before. This effect can be seen on the right side of Fig. 7, where fluorescence signal from vertical line irradiation (= second irradiation event) is lacking in those cells where a horizontal line irradiation (= first irradiation event) was performed (upper part of the image), while it is clearly detectable in cells that were not pre-irradiated (lower part). This effect may be due to limited resources of 53Bp1 protein within the cell nucleus so that damage sites stand in “competition” for the available protein.

#### References

- [1] P. Reichart, G. Datzmann, A. Hauptner, R. Hertenberger, C. Wild, G. Dollinger, *Science* **306**, 1537 (2004).
- [2] A. Hauptner, S. Dietzel, G.A. Drexler, P. Reichart, R. Krücken, T. Cremer, A.A. Friedl, G. Dollinger, *Radiat. Environ. Biophys.* **42**, 237 (2004).
- [3] J.F. Ziegler, J.P. Biersack, <http://www.srim.org>.
- [4] ROOT (An Object-Orientated Data Analysis Framework), <http://root.cern.ch>.
- [5] V. Hable, Diploma thesis, TU München, Physik Department, 2004.